

R. H. YOON\*  
R. Q. HONAKER\*  
G. H. LUTTRELL\*

## APPLICATION OF THE SELECTIVE HYDROPHOBIC COAGULATION PROCESS FOR UPGRADING CARBONACEOUS MATERIAL

It has been shown that naturally hydrophobic carbonaceous materials such as coal and graphite can be selectively coagulated and separated from hydrophilic impurities without using oily agglomerants, flocculants or electrolytes. The coagulation occurs at  $\zeta$ -potentials significantly higher than those predicted by the classical DLVO theory, suggesting that it is driven by the hydrophobic interaction. In the present work, the energy barriers for the coagulation of a hydrophobic coal sample have been calculated using the extended DLVO theory which incorporates the hydrophobic interaction energy in addition to the dispersion and the electrostatic energies. For the coagulation of minerals present in the coal, the classical DLVO theory has been used for the energy barrier calculation. The results of these calculations provide an excellent correlation with the results of a series of Selective Hydrophobic Coagulation (SHC) tests conducted with run-of-mine coal and graphite samples.

### INTRODUCTION

The classical DLVO theory [1-2] has been used extensively for describing the stability of lyophobic colloids. It states that the potential energy ( $V_T$ ) of interacting particles is given by the sum of the repulsive electrostatic interaction energy ( $V_E$ ) and the attractive London-van der Waals dispersion energy ( $V_D$ ) as follows:

$$V_T = V_E + V_D, \quad (1)$$

in which

$$V_E = \frac{\epsilon a \psi_d^2}{2} \ln[1 + \exp(-\kappa H)], \quad (2)$$

and

$$V_D = - \frac{aA_{131}}{12H}, \quad (3)$$

\*Virginia Center for Coal and Minerals Processing, Virginia Polytechnic Institute and State University Blacksburg, Virginia

where  $A_{131}$  is the Hamaker constant for two spheres of 1 in a medium 3,  $a$  the radius,  $H$  the separation distance,  $\epsilon$  the dielectric constant,  $\Psi_d$  the Stern potential, and  $\kappa$  is the Debye reciprocal length. Methods for determining the various parameters of Equations (2) and (3) have been described in literature [3-6].

While the classical DLVO theory is useful for describing the stability of moderately hydrophilic and weakly hydrophobic particles, it fails with very hydrophobic particles. Xu and Yoon [7-8] have shown that unoxidized bituminous coals can be coagulated under conditions of high  $\zeta$ -potentials, indicating that there may be an additional attractive energy other than  $V_D$ . Thus, the classical DLVO theory has been extended as follows:

$$V_T = V_E + V_D + V_H, \quad (4)$$

in which  $V_H$  represents the additional attractive energy associated with the hydrophobic particles. This hydrophobic interaction energy has been expressed in terms of the non-dispersion component of the work of adhesion ( $W_a^{nd}$ ) of water on a solid of interest as follows:

$$V_H = \frac{aD_0C_m}{2(1 + \exp[b(W_a^{nd} - K)])} \exp\left(-\frac{H}{D_0}\right), \quad (5)$$

in which  $C_m$ ,  $b$  and  $K$  are empirical fitting parameters and  $D_0$  is the decay length. Assuming that  $D_0 = 10.3$  nm, Xu and Yoon [11] determined the values of these fitting parameters by conducting coagulation experiments with particle suspensions of different hydrophobicities.

Based on the extended DLVO theory embodied in Eqs. (4) and (5), a process of separating hydrophobic particles from hydrophilic ones has been developed. In this process, which is referred to as selective hydrophobic coagulation (SHC), hydrophobic particles are selectively coagulated while hydrophilic particles are kept in suspension. The separation can be achieved normally by simple pH control without using an agglomerant. In this communication, examples of using the SHC process for cleaning fine coal and graphite are given, while the theoretical basis of the process is also discussed.

## EXPERIMENTAL

SAMPLE: A majority of the SHC tests was conducted using a

run-of-mine Elkhorn No. 3 seam coal, assaying 12.0% ash and 0.81% sulfur. A number of different coal samples was also used in batch SHC tests. As soon as each sample was received, it was crushed to -6 mm using a laboratory jaw crusher. The crushed coal was then split into representative lots of 1,000 grams each, placed into air-tight containers, and stored in a freezer at  $-20^{\circ}\text{C}$  to minimize oxidation.

For the contact angle measurements, chunky specimens of the Elkhorn No. 3 coal were obtained by heavy medium separation using magnetite. The low-gravity fraction was washed with distilled water and air-dried. The samples were cut by a diamond saw and wet-polished using 6-, 3-, and  $1/4\text{-}\mu\text{m}$  diamond pastes on a Texmet-covered disk. The final polishing was done on a microcloth-covered disk with  $0.05\mu\text{m}$  alumina. A part of the precleaned coal samples were ground to -400 mesh for  $\zeta$ -potential measurements.

Amorphous and crystalline graphite samples were obtained from Kyerim Graphite Company and Kumam Graphite Company, Korea, respectively. The amorphous graphite sample was a flotation product containing 17.0% ash and 81.03% fixed carbon. The crystalline graphite sample was a run-of-mine ore containing 85.26% ash and 11.91% fixed carbon. Both samples were 100% finer than 200 mesh. They were split into representative lots of 1,000 grams each using a laboratory splitter.

A pure -5  $\mu\text{m}$  silica sample was acquired from United States Silica, Berkeley Springs, West Virginia for both coagulation efficiency and  $\zeta$ -potential measurements. Kaolin samples were obtained from Fisher Scientific for the same purpose.

**BATCH SHC TEST:** Prior to each experiment, a 1,000 gram coal sample was dry-pulverized in a laboratory hammer mill to -100 mesh. This procedure was followed by wet-grinding at 30% solids in a 13.3-cm diameter Szegvari stirred ball mill using 3.2-mm diameter stainless steel balls. Each sample was micronized for 30 minutes resulting in a mean particle diameter of approximately 5  $\mu\text{m}$ . The samples were then diluted to an appropriate pulp density (0.5-3.0%) in a conditioning sump. The pH of the slurry was adjusted to a desired value by adding either sodium hydroxide or hydrochloric acid.

A 1,000 ml slurry was agitated for 5 minutes at 750 rpm using a 3-inch serrated disk impeller. The mixing vessel was made of 6-inch diameter Plexiglas equipped with four  $1/2$ -inch baffles equally spaced along the inside walls. After agitation, the slurry was let to stand for 5 minutes to allow for coagula growth and sedimentation. The supernatant containing the dispersed mineral matter was siphoned off, leaving the settled coagula in the container. If necessary, the coagula were redispersed by adding more water and the above procedure was repeated.

several times to obtain a desired product quality.

**COAGULATION EFFICIENCY MEASUREMENTS:** The effect of pH on the coagulation of kaolin and silica was studied by determining the coagulation efficiency in the same manner as described by Xu and Yoon [7-8]. Each experiment was conducted by suspending 10 grams of the sample in a 500-ml KCl solution ( $10^{-3}$  M), and agitating it for 5 minutes at 750 rpm. The mixing tank was made of a 3 1/2 inch diameter Plexiglass cylinder equipped with 4 baffles and a 1 3/4 inch diameter variable-speed impeller. After agitation, the suspension was allowed to settle for 3 minutes and 300 ml of the supernatant was removed by siphoning. The solids in the supernatant were weighed after filtration and drying. The coagulation efficiency,  $E_c$ , was calculated as

$$E_c = 100(W_i - W_f)/W_p \quad (6)$$

where  $W_i$  is the initial weight of solids in the supernatant prior to coagulation and  $W_f$  is the weight after coagulation.

**ELECTROKINETIC STUDIES:** The  $\zeta$ -potential measurements were conducted using a Pen-Kem Model 501 Lazer Zee meter. The suspension was prepared by adding 0.02 grams of sample to a 500 ml KCl solution ( $10^{-3}$  M). Sodium hydroxide or hydrochloric acid was added to adjust the pH to a desired value. At least three measurements were taken and averaged for each sample.

**CONTACT ANGLE MEASUREMENT:** Contact angles were measured using a Rame-Hart contact angle goniometer. The sessile drop technique was employed in a closed container to conduct these measurements under equilibrium vapor pressure. An average of 10 measurements was obtained at different sites and specimens and averaged.

## RESULTS

Figure 1 shows the results of a series of SHC tests conducted on the run-of-mine Elkhorn No. 3 seam coal using double-distilled water. At pH 3-8, both coal and mineral matter coagulated, resulting in high combustible recovery and high ash content in the settled coagula. At pH 8-9, only the coal coagulated, while the mineral matter was dispersed, resulting in high combustible recovery and low ash content in the settled coagula. A further increase in pH resulted in a sharp drop in coal recovery, because coal particles began to be dispersed as the pH was increased above 9. Thus, the SHC process has a rather narrow window of selectivity at pH 8.5-9.5.

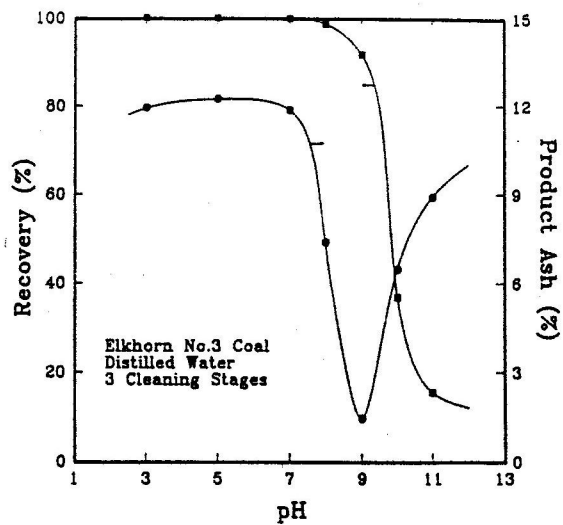


Fig.1.

The effect of pH on combustible recovery and product ash content using an Elkhorn No.3 seam coal (12% ash) in distilled water.

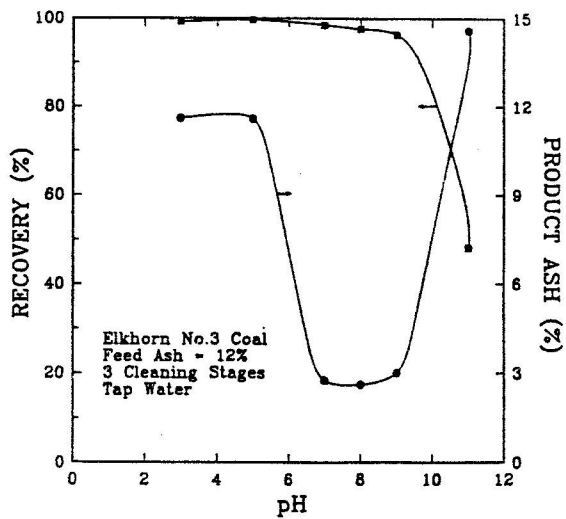


Fig.2.

The effect of pH on combustible recovery and product ash content using an Elkhorn No.3 seam coal (12% ash) in tap water.

The results obtained using tap water (Figure 2) showed a similar trend except that the window of selectivity was pH 7-9, which was significantly broader than the case of using distilled water. This may be attributed to the changes in the coagulation behavior of clays due to the presence of hydrolyzable cations in tap water, as will be discussed further in the later part of this section.

Table 1 shows the results obtained with various coal samples after multiple stages of batch SHC experiments. The coal samples were ground in a stirred ball mill to 3- to 5- $\mu\text{m}$  mean volume size ( $d_{50}$ ). The product ash contents varied in the 0.36-7.5% range depending on the feed ash, degree of liberation, hydrophobicity and the number of cleaning stages employed. The pyritic sulfur rejection varied from 57 to 88%. With the Elkhorn No.3 coal, which assayed 12% ash and 0.25% pyritic sulfur in the feed, the product assayed only 0.03% pyritic sulfur. In general, the SHC process gave very high combustible recoveries for all the coal samples tested. Most of the test results shown in Table 1 were obtained using tap water; however, deionized water was used for the Pittsburgh No. 8, Illinois No. 6, and Upper Freeport coals. No hydrocarbon oils were used in any of the tests.

Table 1.

Results obtained with Various Coal Samples in Batch SHC Tests.

Coal Seam	Ash (%)		Pyritic Sulfur (%)		Combustible Recovery (%)
	Feed	Product	Feed	Product	
U. Cedar Grove	24.0	5.13	----	----	89.2
U. Cedar Grove	12.0	2.45	----	----	91.1
U. Cedar Grove	3.40	0.98	----	----	93.0
L. Cedar Grove	1.44	0.36	----	----	79.1
Elkhorn No.3	12.0	1.14	0.25	0.03	85.3
Elkhorn No.3	5.25	1.34	----	----	93.9
RL-Coal	5.50	1.84	0.65	0.28	90.5
Upper Freeport	12.0	4.84	1.25	0.41	88.5
Illinois No.6	12.0	4.49	1.72	0.55	92.4
Pittsburgh No.8	14.4	3.45	2.31	0.46	88.1
Splashdam	3.50	2.07	----	----	99.1

In addition to coal, crystalline and amorphous graphite samples were upgraded using the SHC process. The separation of the graphite coagula was accomplished using a continuous screening device. The mean volume particle size of both samples was approximately 3  $\mu\text{m}$ , as measured using an Elzone 80-xy particle size analyzer. The tests were conducted at pH 10 and at 2% solids. As shown in Table 2, the ash content of the run-of-mine crystalline graphite was reduced from 85.26% to 7.68%, while maintaining a high fixed carbon recovery of 92.37% after three cleaning

stages. The ash content of the amorphous graphite, which was a flotation product, was reduced from 17.0% to 5.36%. The fixed carbon recovery for the amorphous graphite remained remarkably high, at 99.86%. The tests conducted with both amorphous and crystalline graphite samples produced tailings with high ash contents, indicating the high separation efficiency of the SHC process.

Table 2

Results obtained with Graphite Samples in Continuous SHC Tests

Graphite Type	Cleaning Stage	Ash (%)		Fixed Carbon (%)	Fixed Carbon Recovery (%)
		Product	Tailings		
Amorphous	Feed	17.0	---	81.0	---
	First	8.21	99.1	89.7	100.0
	Second	6.53	98.7	91.1	100.0
	Third	5.36	81.4	91.8	99.9
Crystalline	Feed	85.3	---	11.9	---
	First	38.4	98.1	59.2	100.0
	Second	17.3	86.1	79.0	94.3
	Third	7.68	78.9	86.9	92.4

#### DISCUSSION

As shown in Figure 1, coal particles can be readily coagulated at pH as high as 9. At this pH, the  $\zeta$ -potential of the Elkhorn No. 3 seam coal was found to be -43 mV, from which one can calculate  $V_E$  using Eq. (2). From the Hamaker constant ( $A_{11}$ ) of the coal sample obtained using the methylene iodide contact angle technique [3], the complex Hamaker constant ( $A_{131}$ ) for the coal particles interacting in water was determined to be  $8.68 \times 10^{-24}$  J using the method described by Bargeman et al [4]. This value was used for determining  $V_D$  using Eq. (3). Substituting  $V_E$  and  $V_D$  obtained as such into Eq. (1), the maximum energy barrier ( $V_{T, \max}$ ) can be calculated to be 2,942 kT, which is much too large as compared to the kinetic energies (approximately 60 kT) of the particles involved in the SHC process [9]. This finding suggests that the classical DLVO is not adequate for describing the coagulation of very hydrophobic particles, and needs to be extended by incorporating the hydrophobic interaction energy term ( $V_H$ ), as shown in Eq. (4).

Xu and Yoon [7-8] related  $V_H$  with the non-dispersion component of the work of adhesion ( $W_a^{nd}$ ) of water on different solids, as shown in Eq. (5). For the Elkhorn No.3 coal, ( $W_a^{nd}$ ) was determined to be 33.68 ergs/cm<sup>2</sup> from the values of water contact angle ( $\theta_v = 67^\circ$ ) and the

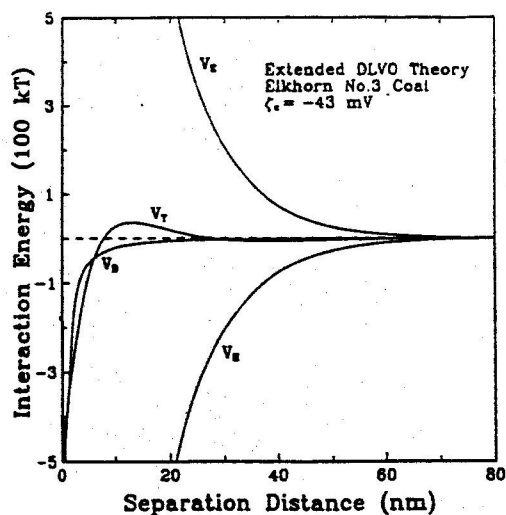


Fig. 3. Interaction energy profile as a function of separation distance for Elkhorn No.3 coal under the following conditions:  $10^{-3}$  M KCl,  $\Psi_d = -43$  mV,  $A_{131} = 8.686 \times 10^{-21}$  J,  $a = 2.5 \mu\text{m}$ , and  $W_a^{nd} = 33.68$  ergs/cm<sup>2</sup>.

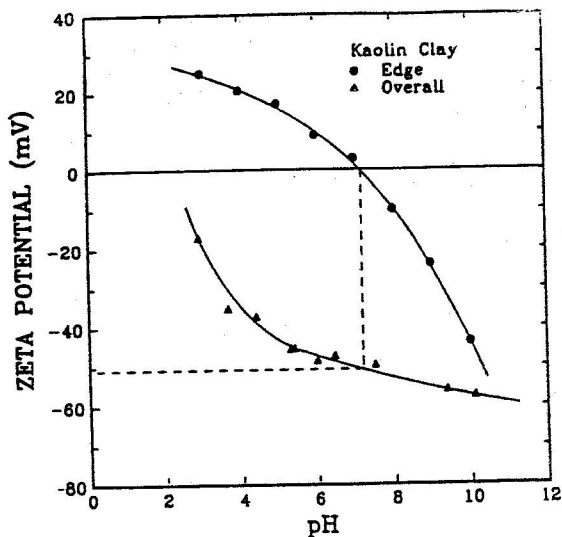


Fig. 4.  $\zeta$ -potentials of the kaolinite (▲) and the calculated  $\zeta$ -potentials of the edge surface (●). The dotted lines show the method of locating the  $\zeta$ -potential of the face;  $10^{-3}$  M KCl.



dispersion component of the surface free energy ( $\gamma_s^d = 50.05 \text{ ergs/cm}^2$ ). By assuming that  $D_o = 10.3 \text{ nm}$ , one can determine  $V_H$ , which can then be substituted to Eq. (4) to obtain an extended DLVO plot (Figure 3). As shown,  $V_{T, \max}$  is approximately 30 kT, which is comparable to the kinetic energies of the particles involved. Figure 3 also shows that  $V_H$  and  $V_E$  play the dominant role in determining the stability of the Elkhorn No. 3 seam coal.

While it is necessary to use the extended DLVO theory for calculating the potential energies between coal particles, the classical DLVO theory may still be useful for interactions involving mineral matter. Therefore, a series of DLVO calculations was made using Eqs. (1)-(3) for interactions involving pure silica, kaolin clay and coal. For homocoagulation of mineral matter, Eq.(2) was used for calculating  $V_E$ , while the constant surface potential model of Hogg, et al. [6] was used for heterocoagulation. For the coagulation involving clay,  $V_E$  was calculated by considering three different cases, i.e., face-to-face, edge-edge and face-to-edge interactions, using the constant surface charge [10], constant potential [6] and mixed [11] models, respectively.

In calculating  $V_E$ ,  $\Psi_d$  was substituted by  $\zeta$ -potentials as an approximation. Figure 4 shows the variation of the  $\zeta$ -potentials at the edge surface of clay (kaolinite) with pH [12]. On the other hand, the  $\zeta$ -potential at the face (basal) surface of kaolinite was assumed to be constant throughout pH range studied. The  $\zeta$ -potential of the kaolinite at the iso-electric point (i.e.p.) of the edge surface (-51 mV) was taken as that at the face surface.

In the DLVO calculations involving silica and kaolinite,  $V_D$  was calculated using appropriate values of Hamaker constants from literature [7, 13]. The calculations were carried out over the pH range of 3 to 11. Figure 5 shows the  $V_{T, \max}$  values for silica in the pH range studied. They provide an excellent correlation with the results of the coagulation efficiency measurements conducted on the silica sample; the coagulation efficiency was virtually zero above pH 4, where  $V_{T, \max}$  reaches 1,700 kT.

The  $V_{T, \max}$  values obtained for clay are shown in Figure 6. For the case of edge-to-edge interaction, it reaches a minimum at the i.e.p. (pH 7.2) of the edge surface. For the case of face-to-edge interaction, on the other hand,  $V_{T, \max}$  is zero below pH 7.2 and increases sharply above this pH. The energy barrier for the face-to-face interaction is not given in Figure 6 as its value (16,000 kT) is too large to be of any significance in coagulation. The  $V_{T, \max}$  values obtained from the DLVO calculations correlate well with the coagulation efficiency measurements conducted with the kaolin sample. The efficiency is shown to decrease

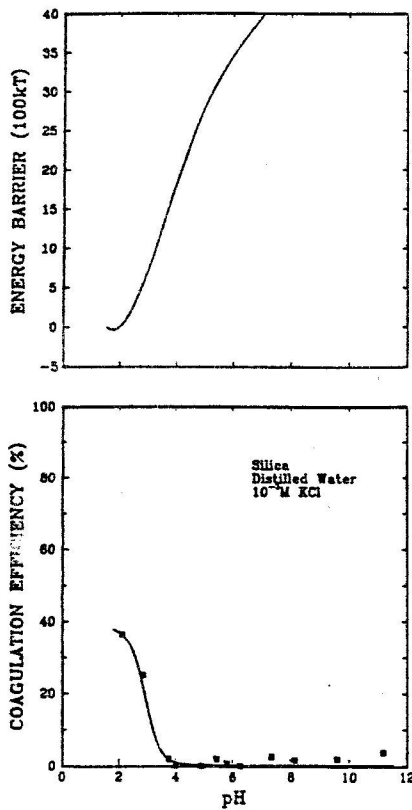


Fig. 5. Calculated  $V_{T, \max}$  values and coagulation efficiency measurements as a function of pH for silica conducted under the following conditions:  $10^{-3}$  M KCl,  $A_{131} = 2.612 \times 10^{-20}$  J, and  $a = 2.5 \mu\text{m}$ .  $\zeta$ -potential versus pH values were: 0, 1.8; -30.3; -38.4, 4; -48.5; -51.6; -55.7; -58.8; -62.9; and -64.10.

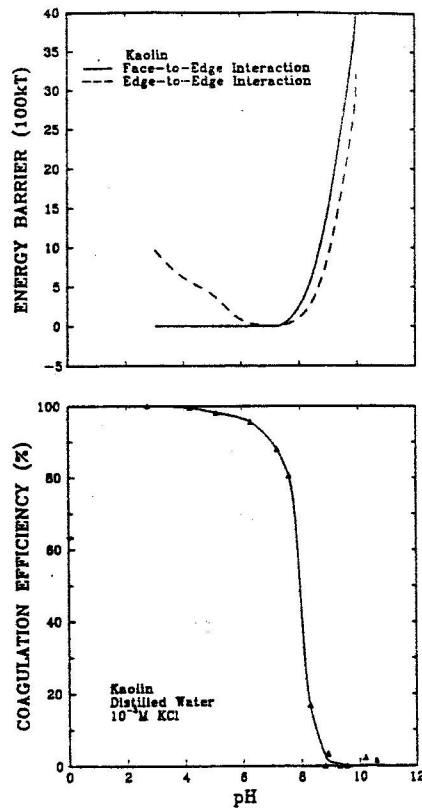


Fig. 6. Calculated  $V_{T, \max}$  values and coagulation efficiency measurements as a function of pH for kaolin conducted under the following conditions:  $10^{-3}$  M KCl,  $A_{131} = 2.01 \times 10^{-20}$  and  $a = 2.5 \mu\text{m}$ .

sharply above pH 7.2, where the energy barrier increases sharply.

Figure 7 compares the results of the SHC tests obtained with the Elkhorn No. 3 seam coal with the  $V_{T, \max}$  values calculated using the

classical and extended DLVO theories. The energy barriers were calculated for all possible combinations of homo- and heterocoagulations. Note that the decrease in combustible recovery at pH 9.5 corresponds closely to the pH where  $V_{T, \max}$  begins to increase significantly; obviously, the decrease in recovery is due to dispersion. Note also that the product ash content begins to increase sharply as the pH decreases below approximately 8.5, which corresponds to the pH where  $V_{T, \max}$  decreases significantly, to below approximately 60 kT for the cases involving the edge surfaces of clay. Therefore, the increase in product ash content can be attributed to the coagulation of clay along with that of coal. Thus, the window of selectivity lies between pH 8.5 and 9.5, with the upper limit dictated by the dispersion of coal and the lower limit determined by the coagulation of clay.

Apparently, the coagulation involving the edge surfaces of clay is most important in determining the selectivity of the process. Apparently, the coagulation involving silica and face surfaces of clay are not as important, because the energy barriers are too large to warrant significant coagulation. Therefore, one can control the selectivity of the SHC process by controlling the surface chemistry of the edge surfaces. Recall that the window of selectivity was considerably broader when tap water was used as compared to the case of using distilled water (Figures 1 and 2). It is possible that some of the hydrolyzable cations present in tap water specifically adsorb on the edge surfaces of the clay and shift the point of zero charge (p.z.c.) to a lower pH, which in turn shifts the  $V_{T, \max}$  versus pH curve to a lower pH.

The hydrophobic coagulation phenomenon has an important implication to flotation kinetics as well. In general, the flotation rate decreases with decreasing particle size (14). This problem can be alleviated if the particle size is enlarged by hydrophobic coagulation. Experiments conducted with micronized coals showed that the  $d_{50}$  size can be increased from approximately 5 to 50  $\mu\text{m}$  due to hydrophobic coagulation.

#### SUMMARY AND CONCLUSIONS

1. Experimental studies carried out in the present work showed that Elkhorn No. 3 coal can be coagulated at  $\zeta$ -potentials as high as -43 mV due to the presence of an attractive hydrophobic interaction energy. This phenomenon has been explained using the extended DLVO theory incorporating the hydrophobic interaction energy.
2. The additional attractive interaction energy associated with hydrophobic particles can be exploited for separating them from

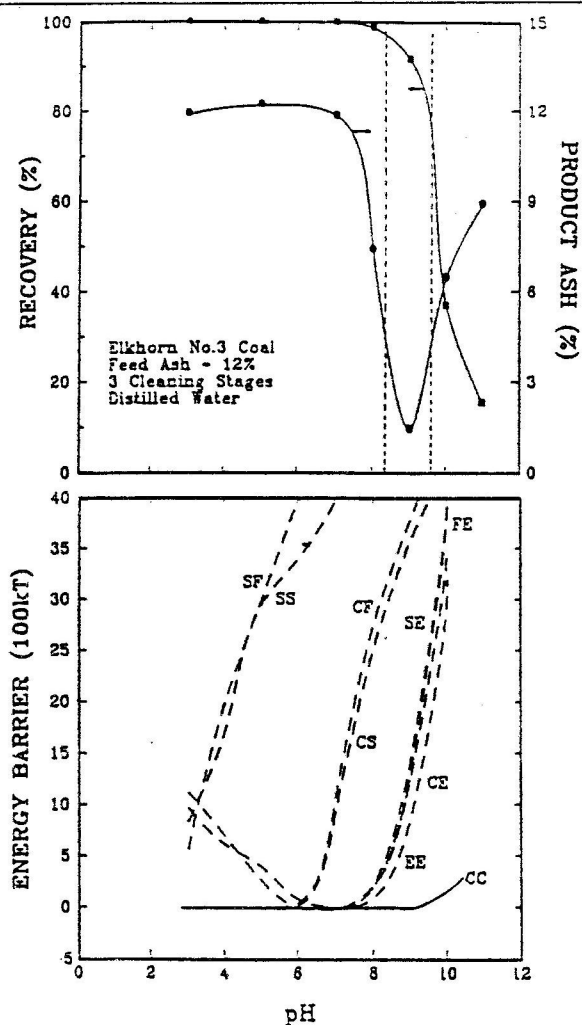


Fig. 7.

Recovery, product ash content, and calculated energy barrier values for the various interactions in the SHC process: Coal-Coal (CC), Coal-Silica (CS), Coal-Clay Edge (CE), Coal-Clay Face (CF), Clay Edge-Clay Edge (EE), Clay Face-Clay Edge (FE), Silica-Silica (SS), Silica-Clay Face (SF), and Silica-Clay Edge (SE).

hydrophilic particles by selective hydrophobic coagulation. The coagula can be separated from the dispersed hydrophilic particles by simple screening or sedimentation techniques.

3. The selective hydrophobic coagulation process has been tested for upgrading coal and graphite. The maximum selectivity of the process can be achieved at a pH between 8 and 9. The upper limit is dictated by the dispersion of coal while the lower limit is determined by the coagulation of clay involving its edge surfaces.

### ACKNOWLEDGEMENT

The authors acknowledge the financial support of the U.S. Department of Energy (Contract No. DE-AC22-90PC90174) and discussions with Dr. Z. Xu.

### REFERENCES

1. Derjaguin, B.V., and Landau, L., *Acta Physicochim. USSR* 14, 633 (1941).
2. Verwey, E.J.W., and Overbeek, J.Th., "Theory of the Stability of Lyophobic Colloids". Elsevier, Amsterdam (1948).
3. Fowkes, F.M., *Ind. Eng. Chem.* 56, 40 (1964).
4. Bargeman, D., and Vader, F. Van Voorst, *Electroanal. Chem. Interfacial Electrochem.* 37, 45 (1972).
5. Derjaguin, B.V., *Kolloid Z.* 69, 155 (1934).
6. Hogg, R., Healy, T.W., and Fuerstenau, D.W., *Trans. Faraday Soc.* 62, 1638 (1966).
7. Xu, Z., and Yoon, R.H., *J. Colloid Interface Sci.* 132, 532 (1989).
8. Xu, Z., and Yoon, R.H., *J. Colloid Interface Sci.* 134, 427 (1990).
9. Xu, Z., "A Study of Hydrophobic Interactions in Fine Particle Coagulation". Ph.D.thesis, Department of Mining and Minerals Engineering, Virginia Polytechnic Institute and State University, 1990.
10. Wiese, G.R., and Healy, T.W., *Trans. Faraday Soc.* 66, 490 (1970).
11. Kar, G., Chander, S., and Mika, T.S., *J. Colloid Interface Sci.* 44, 347 (1973).
12. Williams, D.J.A., and Williams, K.P., *J. Colloid Interface Sci.* 65, 79 (1978).
13. van Olphen, H., "An Introduction to Clay Colloid Chemistry." John Wiley & Sons, New York (1977).
14. Ahmed, N., and Jameson, G.J., *Mineral Processing and Extractive Metallurgy Review* 5, 77 (1989).

### Streszczenie

Yoon R.H., Honaker R., Luttrell G.H., 1991, Zastosowanie procesu selektywnej hydrofobowej koagulacji do wzbogacania substancji węglowych. *Fizykochemiczne Problemy Mineralurgii*, 24; 33-45 (tekst angielski)

Wykazano, że naturalnie hydrofobowe substancje jak węgiel i grafit mogą być selektywnie koagulowane i oddzielane od hydrofilnych zanieczyszczeń bez dodatku olejów, flokulantów, czy też elektrolitów. W pracy obliczono barierę energetyczną koagulacji hydrofobowego węgla wykorzystując rozszerzoną teorię DLVO, która uwzględnia obok energii oddziaływań dyspersyjnych i elektrycznych także energię oddziaływań hydrofobowych. Obliczone własności dobrze korelują z wynikami selektywnej hydrofobowej koagulacji dla węgla i grafitu.